Pro-arrhythmic Effects of Increased Late Sodium Current in Failing Human Heart

Jieyun Bai[1], Kuanquan Wang[1], Xiangyun Bai[1], Yongfeng Yuan[1],Henggui Zhang[1,2]

[1]School of Computer Science and Technology, Harbin Institute Technology, Harbin, China
[2]School of Physics and Astronomy, University of Manchester, Manchester, UK

Abstract

Heart failure (HF) induces remodeling in cellular ionic channel kinetics, calcium and sodium cycling in the ventricle. In the present study, we investigated the effects of late Na^+ current (I_{NaL}) on rate-dependent electrical activity of failing human ventricle by characterizing rate-dependent I_{NaL} and $[Na^+]_i$, action potential duration (APD) prolongation, and early afterdepolarizations (EADs). Transmural ventricular APD dispersion and conduction velocity restitution (CVr) of 1-D virtual tissue were also investigated. In addition, the developed model was used to simulate ventricular electrocardiograms (ECG) under normal and HF conditions by using a 2-D idealized model. The results were in good accordance with experimental observations: under the HF condition, enhanced I_{NaL} contributed to the reverse rate-dependent (RRD) effects, APD prolongation and EADs generation in cells, and increased dispersion of APD and slowed down conduction in 1-D tissue. ECGs under normal and HF conditions were compared, demonstrating the importance of enhanced I_{NaL} which could be responsible for the increased arrhythmia susceptibility in human HF.

1. Introduction

Patients with congestive HF are prone to develop complex ventricular tachyarrhythmias, which may lead to sudden death. Thus, understanding the mechanisms of initiation of cardiac arrhythmias is of great importance for practical cardiology. Unfortunately, the exact mechanisms by such arrhythmias occur in the failing human heart are incompletely understood yet. Experimental studies conducted with animal models of HF have shown that ventricular arrhythmias are mainly due to non-reentrant mechanisms, most likely due to triggered activity arising from afterdepolarizations [1]. It has been postulated that abnormal cellular electrical activities may give rise to arrhythmias in heart failure, but the proof for this hypothesis remains lacking.

Recent studies have found that the increase of I_{NaL} constitutes an important factor in APD prolongation, variability and EADs generation [2-4]. However, it is still unclear how I_{NaL} affects the rate-dependent electrical activity and thus ventricular excitation conduction in failing human. The I_{NaL} is normally small in normal heart, but can be proarrhythmic when enhanced or when cardiac repolarization reserve is reduced by I_{Kr} blockers [5]. In this study, we investigated rate-dependent properties of I_{NaL} and its impact on arrhythmic risk under HF conditions.

2. Methods

We simulated HF in cells and a 1-D transmural ventricular strand using an existing OVVR model for human ventricular action potentials [6]. To simulate HF, the OVVR model for endo- cardial cells was modified to incorporate HF-induced ion channel remodeling following the study of Trenor et al. [7], which were based on experimental data observed in failing human hearts. To simulate the effects of enhanced I_{NaL} in human HF, the OVVR model was further modified to incorporate data used in the formulation of I_{NaL} from Maltsev et al. [8], the mean time constant ($\tau_{h,L}$>600ms) and the current density increase by 200% and 23% in failing human hearts[9].

The cell models were then incorporated into a reaction diffusion partial differential equation (PDE) of 1-D virtual tissue, which takes the form:

$$C_m \frac{dV_m}{dt} = -I_{tot} + D \cdot \frac{\partial^2 V}{\partial^2 x} \quad (1)$$

where D is the diffusion constant with value 0.1171 (mm^2/ms) to give a conduction velocity of 38.2 cm/s for a solitary wave in a 1-D endo- tissue. A time step 0.02 (ms) and a space step 0.15 (mm) were taken to obtain stable numerical solutions. The virtual ventricular strands were taken to be 15 mm in length in accordance with the physiological thickness of the ventricular wall. The ratio is 25:35:40 for endo-, mid- and epi- cells in the model.

The ECG (pseudo-ECG) formulation was computed as the followings [11]:

$$ECG=\int \frac{D\Delta V_m \cdot \vec{r}}{r^3} dV$$
$$r=\sqrt{(x-x_0)^2+(y-y_0)^2} \quad (2)$$

where V is the area of 2D ideal tissue, $\vec{r}$ the vector from the recording electrode (x_0, y_0) to a point in the tissue (x, y), and r the distance of the two points. (x_0, y_0) is the coordinates of the electrode. In this paper, we placed the virtual electrode in the middle of the model at the right side, 2 cm distance off the epi- layer.

Biomarkers were measured and calculated from endo- cellular and transmural strand simulations under different conditions, which included: APD_{90}, as the APD at 90% repolarization, spatial gradient of APD_{90}, as the change rate of two adjacent cells' APD_{90}, conduction velocity (CV), as the wavefront propagation velocity.

Rate-dependent I_{NaL} curves were obtained by varying PCL. Rate-dependent $[Na^+]_i$ curves were generated at various stimulation rates under different conditions by using a staircase protocol. CV restitution curves were obtained by varying PCL and plotting CV against PCLs.

All measurements were analyzed after achieving steady state conditions, with a BCL of 1000 ms.

3. Results and discussion

3.1. Cell simulation

Rate-dependent I_{NaL} and $[Na^+]_i$: The QT interval represents electrical depolarization and repolarization of the ventricles. A lengthened QT interval is a marker for the potential of ventricular tachyarrhythmias like torsades de pointes and a risk factor for sudden death. In order to reveal the ionic basis that I_{NaL} contributed to the QT lengthening, particularly at the slow rate, we calculated the I_{NaL} current of the endo- cell at different BCLs under the normal condition. As showed in Figure 1, with an increased BCL, the I_{NaL}'s peak was increased and its activation duration during the time course of action potential was prolonged. Such a rate-dependent effects on I_{NaL} became more significant when I_{NaL} was enhanced (I_{NaL} was doubled with CL=4000ms).

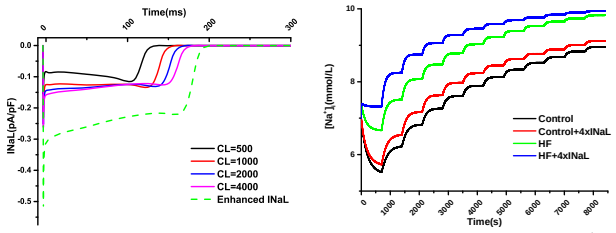

(A) Rate-dependent I_{NaL} (B) Rate-dependent $[Na^+]_i$

Figure 1. I_{NaL} (A) and $[Na^+]_i$ (B) representation of rate-dependent effects in different BCLs are compared.

Time course of $[Na^+]_i$ under HF conditions at various stimulation rates were also investigated using a staircase protocol. In the HF condition, the computed $[Na^+]_i$ had higher concentration as compared to the control condition regardless of the stimulation rate, as shown in Figure 1(B). This was consistent with experimental data of Pieske et al. [12] obtained in failing human myocardial cells. Higher $[Na^+]_i$ limits forward-mode and favors reverse-mode Na-Ca exchanger (NCX), which disturbed Ca^{2+} handling in the failing heart.

APs in failing human: APD prolongation is considered a hallmark change in the failing myocardium [15]. Our simulation data showed that APDs in the HF condition were significantly longer than those in the control condition (Figure 2(A)). Such APD prolongation was further augmented with an increased I_{NaL}, especially under the HF condition. As shown in Figure 2(C), enhanced I_{NaL} or reduced I_{Kr} resulted in a marked APD prolongation. In the HF condition, an integral action of enhanced I_{NaL} and 50% inhibition of I_{Kr} produced EADs, which could be proarrhythmic[13]. Note that under the HF condition, APD prolongation in the mid- cell was significantly greater than other two type cells (Figure 2(B)), which may result in increased transmural heterogeneity. In addition, in the mid-cell, EADs were generated when I_{NaL} was four-fold increased without I_{Kr} inhibition (Figure 2(D)), suggesting it was more prone to EAD genesis as compared to endo- and epi-cells.

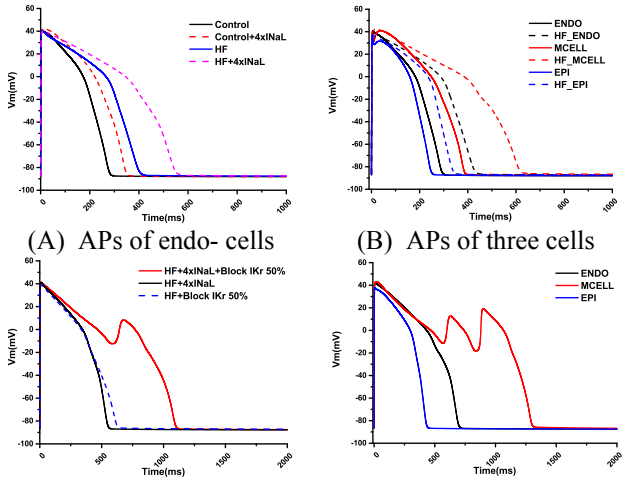

(A) APs of endo- cells (B) APs of three cells

(C) EADs of endo- cells (D) EADs of mid- cells

Figure 2. Simulated EADs with enhanced I_{NaL}. (A) APs were prolonged with increase of I_{NaL} (B) Simulated APs for endo-, mid- and epi-cardial cells in control and HF conditions. HF produced the largest APD prolongation in the mid-cell. . (C) Integral effect of HF-induced ion channel remodelling, I_{Kr} blocking (by 50%) and augmented I_{NaL} on APs. EADs was generated when I_{NaL} was four-fold of its original value. (D) EADs was produced in the mid-cell under HF+4xI_{NaL} conditions in the absence of inhibition of I_{Kr}.

3.2. 1-D transmural strand simulation

Transmural ventricular APD dispersion: Further simulations were performed to characterize the effects of HF-induced ion channel remodeling on transmural ventricular APD dispersion and the temporal vulnerability of tissue for genesis of unidirectional conduction block in response to a premature stimulus [16]. Figure 3 showed the computed spatial distribution of APD_{90} (top panel) and the spatial gradient of APD_{90} (bottom panel). Compared with the Control condition, HF increased the APD across the strand, as well as the APD gradient, suggesting a markedly increase in the APD dispersion across the transmural strand, which is potentially pro-arrhythmic.

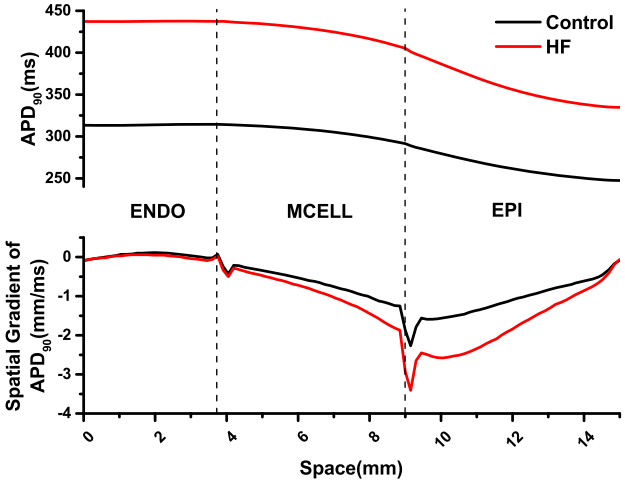

Figure 3. Spatial distribution and actual spatial gradient of APD_{90} in a 1-D transmural strand model of human ventricle for Control (black) and HF (red) conditions. Vertical dotted lines indicate the boundary between different cell types along the strand.

Restitution curve of CV: Abnormal activation delay at rapid activation rate could increase dispersion of conduction and repolarization. To determine the conduction abnormality in the failing human, the rate-dependence of conduction velocity of ventricular excitation waves (CV-R) was computed by using a 1-D endo- strand. Results were shown in Figure 4. It was shown that across the whole range of diastolic interval (DI), the computed CV was dramatically smaller than that in the control condition. This suggested that HF impaired ventricular excitation wave conduction. Such abnormal CV has been shown to contribute to the susceptibility to arrhythmia [14], as conduction delay can cause conduction block leading to the formation of re-entry.

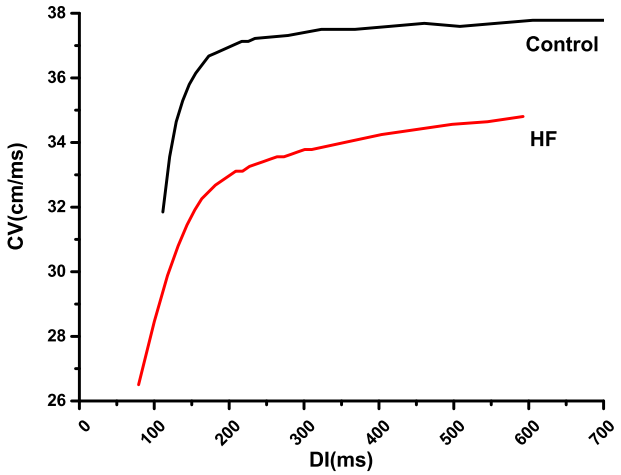

Figure 4. Computed CV-R under control (black) and HF (red) conditions

3.2. ECGs simulation

Clinical studies have suggested in HF patients the ECG has an increased QT dispersion and prolonged interval between the peak and the end of the T-wave, which is associated with dispersion of ventricular repolarization and arrhythmias [14]. To establish the causative link between HF-induced ion channel remodeling and increased repolarization dispersion, we simulated pseudo-ECG waveforms in control and HF conditions by using a 2D idealized model. Results were shown in Figure 5. Compared to the control condition, HF-induced ion channel remodeling caused an increase in the QT dispersion and a prolonged time interval between the peak and the end of T-wave. Our simulation data suggested that the clinical observed changes in the ECG in HF patients can be attributable to the HF-induced ion channel remodeling.

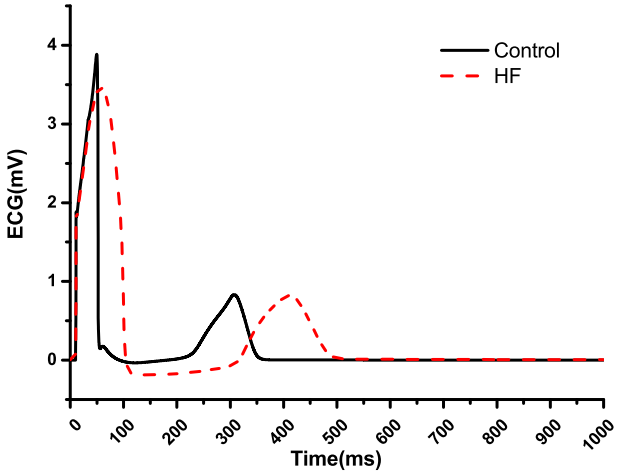

Figure 5. Simulated ECGs in control and HF conditions.

4. Conclusion

In this study, we examined the effects of an enhanced I_{NaL} on ventricular repolarization and conduction of excitation waves in human ventricular models in HF conditions. It was shown that HF produced APD prolongation and slowing down of conduction. It also augmented APD dispersion, which together with impaired ventricular conduction may contribute to increased tissue susceptibility for arrhythmogenesis. Specifically our main findings are: (i) I_{NaL} increased significantly at slow pacing rates and contributed to higher $[Na^+]_i$ as observed in HF condition. High $[Na^+]_i$ limits forward-mode and favors reverse-mode of NCX, which may cause disturbed Ca^{2+} handling as seen in HF [12]; (ii) an increased I_{NaL} is an important factor for APD prolongation, which increases cell's susceptibility to genesis of EADs (reduced I_{Kr} 50%); (iii) an enhanced I_{NaL} increased APD dispersion and APD gradient at some local regions across the transmural strand, which may lead to an increased tissue's vulnerability to the genesis of uni-directional conduction by a premature excitation; (iv) HF produced an abnormal CV restitution curve with a steeper slope, which has been shown to contribute to the susceptibility to arrhythmia; (v) HF increased the QT dispersion and the time interval between the peak and the end of the T-wave. This established a causative link between the increased QT dispersion and HF remodeling as seen in HF patients.

Acknowledgements

This work is supported by the National Natural Science Foundation of China (NSFC) under Grant No. 61179009, No. 61173086 and No. 61001167.

References

[1] Janse MJ. Electrophysiological changes in heart failure and their relationship to arrhythmogenesis. Cardiovasc Res 2004; 61: 208-217.

[2] Song Y, Shryock JC, Belardinelli L. An increase of late sodium current induces delayed afterdepolarizations and sustained triggered activity in atrial myocytes. Am J Physiol Heart Circ Physiol 2008; 294: H2031-H2039.

[3] Valdivia CR, Chu WW, Pu J, Foell JD, Haworth R A, Wolff MR, Makielski JC. Increased late sodium current in myocytes from a canine heart failure model and from failing human heart. J Mol Cell Cardiol 2005; 38: 475-483.

[4] Maltsev VA, Undrovinas A. Late sodium current in failing heart: friend or foe? Prog Biophys Mol Biol 2008; 96: 421-451.

[5] Guo D, Liu Q, Liu T, Elliott G, Gingras M, Kowey PR, Yan GX. Electrophysiological properties of HBI-3000: a new antiarrhythmic agent with multiple-channel blocking properties in human ventricular myocytes. J Cardiovasc Pharmacol 2011; 57: 79-85.

[6] O'Hara T, Virág L, Varró A, Rudy Y. Simulation of the undiseased human cardiac ventricular action potential: model formulation and experimental validation. PLoS Comput Biol 2011; 7: e1002061.

[7] Trenor B, Cardona K, Gomez JF, Rajamani S, Ferrero Jr JM, Belardinelli L, Saiz J. Simulation and mechanistic investigation of the arrhythmogenic role of the late sodium current in human heart failure. PloS One 2012; 7: e32659.

[8] Maltsev VA, Sabbah HN, Higgins RS, Silverman N, Lesch M, Undrovinas AI. Novel, ultraslow inactivating sodium current in human ventricular cardiomyocytes. Circulation 1998; 98: 2545-2552.

[9] Maltsev VA, Silverman N, Sabbah HN, Undrovinas AI. Chronic heart failure slows late sodium current in human and canine ventricular myocytes: implications for repolarization variability. Eur J Heart Fail 2007; 9: 219-227.

[10] Elshrif MM, Cherry EM. A quantitative comparison of the behavior of human ventricular cardiac electrophysiology models in tissue. PloS one 2014; 9: e84401.

[11] Ten Tusscher KH, Bernus O, Hren R, Panfilov AV. Comparison of electrophysiological models for human ventricular cells and tissues. Prog Biophys Mol Biol 2006; 90: 326-345.

[12] Pieske B, Maier LS, Piacentino V, Weisser J, Hasenfuss G, Houser S. Rate dependence of [Na+] i and contractility in nonfailing and failing human myocardium. Circulation 2002; 106: 447-453.

[13] Wu L, Ma J, Li H, Wang C, Grandi E, Zhang P, Belardinelli L. Late sodium current contributes to the reverse rate-dependent effect of IKr inhibition on ventricular repolarization. Circulation 2011; 123: 1713-1720.

[14] Lou Q, Janks DL, Holzem KM, Lang D, Onal B, Ambrosi CM, Efimov IR. Right ventricular arrhythmogenesis in failing human heart: the role of conduction and repolarization remodeling. Am J Physiol Heart Circ Physiol 2012; 303: H1426-H1434.

[15] Aiba T, Tomaselli GF. Electrical remodeling in the failing heart. Curr Opin Cardiol 2010; 25: 29-36.

[16] Akar FG, Rosenbaum DS. Transmural electrophysiological heterogeneities underlying arrhythmogenesis in heart failure. Circ Res 2003; 93: 638-645.

Address for correspondence.
Kuanquan Wang
Mailbox 332, Harbin Institute of Technology
Harbin 150001, China
wangkq@hit.edu.cn